Jour. Geol. Soc. India (2022) 98:1455-1465
https://doi.org/10.1007/s12594-022-2193-9

ORIGINAL ARTICLE

Study on the Hydrogeochemical Processes Regulating the Groundwater Chemistry in the Southeast Rajasthan

Parmeshwar Lal Meena
Department of Chemistry, University of Rajasthan, Jaipur - 302 004, India
E-mail: *parmeshwar1978@gmail.com*

Received: 19 December 2021 / Revised form Accepted: 15 March 2022

ABSTRACT

The current study is focused on evaluation of hydrogeochemical aspects of groundwater for analysis of groundwater chemistry and quality assessment in the south east Rajasthan (India). A total of 50 groundwater samples were collected and analyzed for the assessment of major cations and anions, total dissolved solid (TDS), electrical conductance (EC), total hardness (TH) and total alkalinity (TA), and the results were compared with the WHO standards of drinking water. The results have demonstrated that the groundwater is alkaline in nature and in most of the groundwater samples the quantity of TH, TDS, EC, TA and NO_3^- is exceeded to the WHO standards. Additionally, alkali metal ions are mainly contributed from the dissolution of halite and silicate weathering processes, whereas the alkaline earth metal ions from the carbonate dissolution and silicate weathering processes. The saturation indices (SI) values show that the groundwater in the study area is oversaturated in terms of dolomite, calcite and argonite while undersaturated in gypsum. Hydrogeochemically the groundwater is Ca.Mg-HCO_3, Ca.Mg-Cl and Ca.Mg-SO_4 types. Moreover, it is mixed type with reference to cations and anions. The ionic plots, molar ionic ratios, CAI, SI and Gibb's diagram have revealed that the chemical weathering of rock minerals, reverse ion exchange and anthropogenic activities are the key processes, regulating the chemical composition of ground water in the study area.

INTRODUCTION

Water is the basic need of living beings and it is very critical for the growth of living beings on the earth planet. The availability of safe and clean drinking water is indispensable for the survival of living beings (Kagan et al., 1992). Only 3 % water on the earth is available as fresh water out of which only 0.01% water is accessible for human use. The groundwater is the largest freshwater resource after the glaciers and polar ice in the world that plays very important role in the sustainability of life on the earth. Additionally, it is critical for supporting the socio-economic development and maintaining the healthy ecosystem (Mohammed, 2015). Across the world approximately, 65% of groundwater is used for the drinking purposes, 20% for irrigation and remaining is utilized in industries (Salehi et al., 2018).

Globally, the rapid growth in population, fast rate of industrialization and urbanization activities, and climate change has increased the demand and exploration of groundwater significantly (Green 2016; Tolera 2020). Further, globally the decline of surface water resources and deterioration of surface water quality has also increased the dependence of population on the groundwater resources for drinking and domestic purposes (Raju et al., 2011; Madhav et al., 2018). In the past, as compared to the surface water, the groundwater was considered safer, but nowadays due to the overexploitation, uncontrolled use, and improper waste management have increased pollution load in the groundwater (Iqbal and Gupta, 2009). As a result, the groundwater is adversely affecting and causing higher withdrawal costs (Duraisamy et al., 2018; Qasemi et al., 2019). Today, the quality, quantity and availability of water have become the major sociopolitical and environmental issues across the world (Rossiter et al., 2010).

Restoring the original quality of already contaminated groundwater is very difficult (Duraisamy et al., 2018; Qasemi et al., 2019). The use of contaminated groundwater not only can cause adverse health issues but, also affects the socioeconomic growth of country (Milovanovic, 2007). The quality and hydrogeochemical properties of the groundwater are mainly depend on the local hydrogeology, topography, geological structures, evaporation, precipitation, rock-water interactions, weathering, industrial effluents, agricultural and anthropogenic activities (Adimalla and Venkatayogi, 2018). But, the increased anthropogenic activities are greatly influencing the ground-water chemistry.

The anthropogenic activities that greatly manipulate the groundwater chemistry are dumping of solid waste, domestic and industrial waste, mining and agricultural activities (Hem, 1991). In recent years, many research reports have been published in which the impact of various factors on the hydrogeochemistry of the groundwater have been studied (Gogoi et al., 2021; Wanda et al., 2021; Tiwari et al., 2021). By understanding the hydrogeochemical characteristics of the groundwater in any geographical region, the quality of groundwater for domestic and agricultural purposes can be evaluated.

Hence, it is imperative to assess the hydrogeochemistry of the groundwater for the effective management and utilization of the groundwater resources, assurance of drinking water safety and for the promotion of environmentally sustainable developments (An and Lu, 2018; Appelo and Postma, 2005; Hem, 1991). Furthermore, the hydrogeochemical characterization of groundwater can be useful for revealing the interaction mechanism between groundwater and its surrounding environment, and it may also provide new insights for water protection and management (Li et al., 2015; Qian et al., 2012). The present study area is the part of southeast Rajasthan (India) and situated in semiarid region. The hydrogeochemical studies of groundwater in selected region is not carried out at all, and a little

is known about the geochemical processes, chemical composition of the groundwater and the anthropogenic influences on the groundwater.

Therefore, the current study was taken up to know the hydrogeochemical processes controlling the groundwater chemistry and quality assessment for drinking purpose.

STUDY AREA

Location, climate and Drainage

The study area is a part of Ajmer division in southeast Rajasthan (India). It is located between 25°21'6" N to 25°46'23" N latitude and 75°2'50" E to 75°27'42" E longitude (Fig.1). It experiences a semi-arid climate. The minimum and maximum temperatures are 7.3°C and 46°C, respectively. Atmosphere is generally dry except during the monsoon months (July to September) and the annual rainfall is about 771 mm. 95% of the total annual rainfall is received during the southwest monsoon. Major part of the study area drains into Banas river basin and the south east part contribute to the Chambal river basin (CGWB, 2013).

Topography and Geology

The topography of the study area consists of fairly open plains in the north and southeast with a few hillocks and undulating plains, and hills in the south and northeastern part. The aquifers are formed within the weathered, fractured and jointed hard rock areas. Major water bearing formations are schist and phyllite, schist is the most predominant aquifer type and the aquifers are overexploited (CGWB, 2013). The rocks of this belt are of early Proterozoic and geologically, major part of the study area is occupied by dolomite, phyllite, and quartzite rocks and these rocks consists of quartz, soda feldspar, biotite, potash feldspar, hornblende, actinoite along with zircon and apatite.

MATERIALS AND METHODS

Sampling procedure

In the present study, to evaluate the hydrogeochemistry of groundwater of the south east Rajasthan (India), 50 representative groundwater samples were collected from dug wells, hand pumps and bore wells which were active, functional and water was in regular use for drinking and other domestic purposes. Samples were collected in 1L polyethylene bottles in pre-monsoon season (May, 2019) and before collection of samples, bottles were cleansed with distilled water and subsequently with sampled groundwater. All the samples were preserved at 25°C and transported to the laboratory for further analysis. Sampling, preservation and analysis of water samples were carried out following the method recommended by APHA (1995).

Methodology

Electrical conductivity (EC) and pH of the collected groundwater samples were measured using digital meters immediately after sampling at sites. The groundwater samples collected were analyzed for total dissolved solids (TDS), total alkalinity (TA), total hardness (TH), major cations such as sodium (Na^+), potassium (K^+), calcium (Ca^{2+}), magnesium (Mg^{2+}) and major anions chloride (Cl^-), bicarbonate (HCO_3^-), carbonate (CO_3^{-2}), sulphate (SO_4^{-2}), fluoride (F^-) and nitrate (NO_3^-) in the laboratory using the standard methods recommended by APHA (1995). Calcium (Ca^{2+}) and magnesium (Mg^{2+}) were determined EDTA titration method, chloride (Cl^-) was determined by standard $AgNO_3$ titration, carbonate (CO_3^{-2}) and bicarbonate (HCO_3^-) were determined by titration with HCl. Sodium (Na^+) and potassium (K^+)

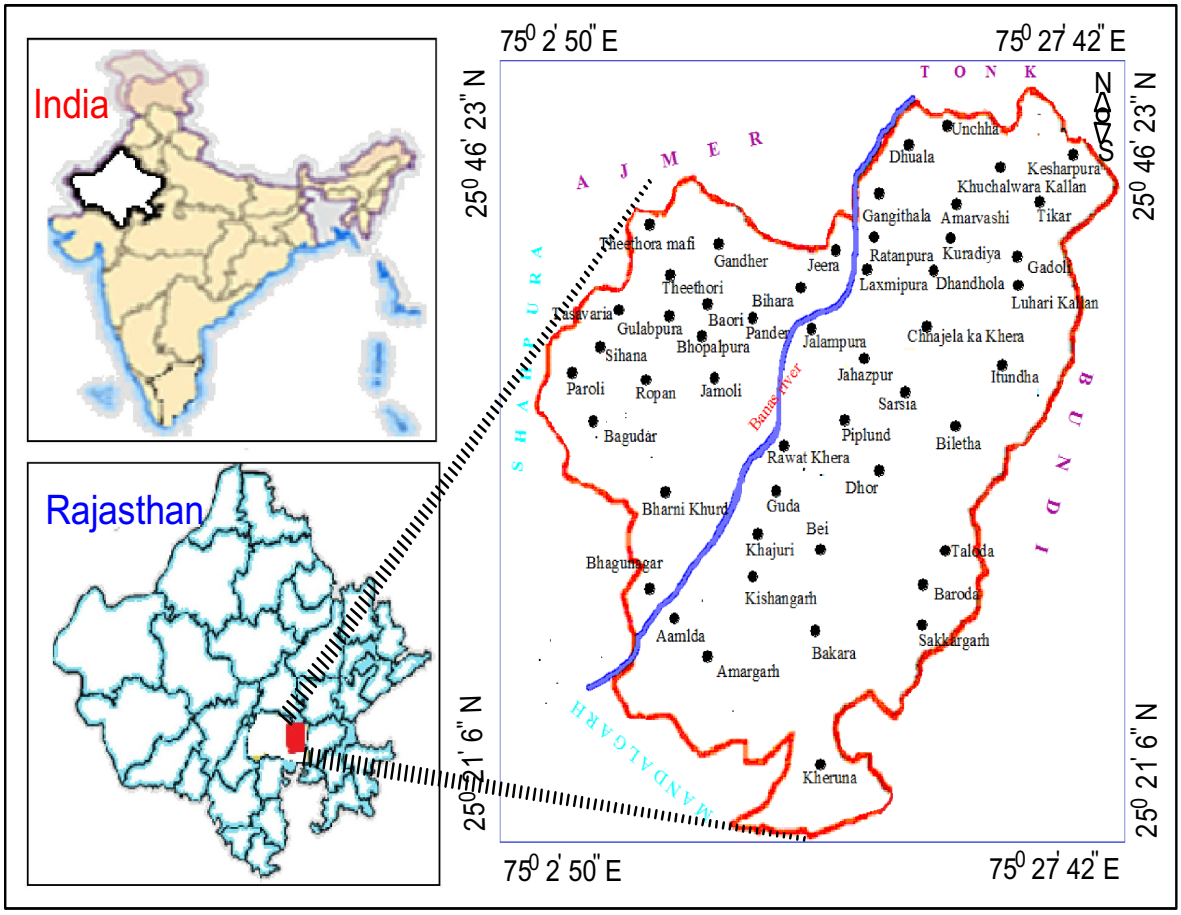

Fig.1. Sampling location map of study area.

were measured by flame photometry. Sulphate (SO_4^{-2}) and nitrate (NO_3^-) were determined by using UV-visible spectro-photometer and an ion-selective electrode was used to determine fluoride (F^-). TDS was calculated from ionic data. Total hardness was calculated by Ca^{2+} and Mg^{2+} data and TA was calculated from Ca^{2+} data. All the analyses were carried out in duplicate and the results were found reproducible within ±5% error limit.

Hydrogeochemical Study of Groundwater

The hydrogeochemical characterization of groundwater in the study area was carried out using diverse molar ionic ratios of ions, ionic relation plots, saturation indices (SI), chloro alkaline indices (CAI) and graphical tools. Water types were identified from analysis of Piper, Chadha, Durov and Scholler diagrams, and the geochemical delineation and controlling factor studies of groundwater were carried out consulting the various molar ionic ratios, ionic relation plots, Gibbs diagrams, CAI and SI values. To draw various plots, diagrams and calculate indices AqAQ Rockware 1.5 demo free software was used. The saturation indices represent the saturation states of minerals in groundwater. Saturation indices (SI) for calcite, dolomite and gypsum minerals were calculated using PHREEQC software. The saturation index (SI) of a given mineral can be defined as SI > 0 signifies oversaturation, SI < 0 signifies undersaturation and SI = 0 signifies equilibrium conditions of the minerals in solution (Langmuir 1997). The chloro-alkaline indices (CAI) values for water samples reflect about the ion exchange reactions between the groundwater and its host environment during residence or travel time. The exchange of Na^+ and K^+ ions from water with Mg^{2+} or Ca^{2+} ions from the sediments increases Mg^{2+} or Ca^{2+} ions concentration in groundwater and the CAI values will be positive, indicateing base exchange reaction, whereas negative values of CAI reflects chloro-alkaline disequilibrium which is also called as cation-anion exchange reaction (Adrian et al., 2007).

RESULTS AND DISCUSSIONS

Groundwater Chemistry and Suitability for Drinking

In order to assess the quality of groundwater for drinking purpose, the determined values of the physicochemical parameters were compared with the prescribed limits of the World Health Organization (WHO, 2011) as depicted in Table 1.

From the results of groundwater analysis it is inferred that the groundwater of the study area is not apposite for direct use for drinking purpose and it need to be treated before the utilization. The major objectionable constituents of the groundwater are TDS, TH, SO_4^{2-}, F^-, Ca^{2+} and Mg^{2+}. The pH values of the groundwater samples range from 7.57 to 8.63 with mean value of 8.09, which indicates that the groundwater is slightly alkaline in nature. The alkaline pH values may

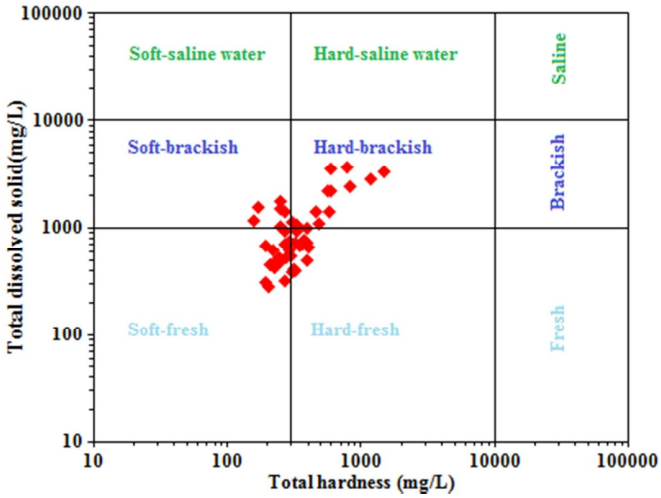

Fig.2. Classification of groundwater based on TDS and TH

be due to the leaching of dissolved constituents into groundwater. The Electrical conductivity (EC) values varied from 392.03 to 5169.74µS/cm with an average of 1536.18µS/cm. In 54% of groundwater samples, EC value is exceeded to the acceptable limit of 1000 µS/cm. High values of EC indicate the presence of high concentration of soluble salts in the groundwater sources and reflect the contribution from mostly geogenic activities.

The total dissolved solid (TDS) values ranged from 274.37 to 3618 mg/L with an average of 1075.11 mg/L, in 74% of the water samples TDS is exceeded to the acceptable limit of 500 mg/L (WHO, 2011). As depicted in Fig. 2, 62% of groundwater samples are categorized as fresh water with TDS <1000 mg /L, and rest of the 38% comprised of brackish water with TDS 1000–10,000 mg/L (Freeze and Cherry, 1979). The salinity load of groundwater in the study area is controlled by Cl^-, TH, Ca^{2+}, Mg^{2+} and NO_3^- that is confirmed from the correlation analysis studies (Table 2).

The total hardness of the groundwater samples ranged from 155.7 mg/L to 1461.55 mg/L with mean value of 374.84mg/L in the study area. 93.6% of the groundwater samples belong to the very hard type of waters, in which TH level is recorded >180 mg/L (Dufor and Becker, 1964).

Among the anions HCO_3^- is dominated followed by Cl^- and SO_4^{2-}. The HCO_3^- concentration is estimated from 49.93 mg/L to 1162.6 mg/L with 233.77 mg/L of average concentration in the groundwater samples. The occurrence order of anions is found to be $HCO_3^- > Cl^- > SO_4^{2-} > NO_3^- > F^-$. The HCO_3^- in the groundwater is mostly derived from the weathering of carbonate and silicate minerals.

Chloride (Cl^-) concentration is from 49.93 mg/L to 1162.6 mg/L

Table 1. Summary of analytical data's for groundwater samples

Parameters	Min.	Max.	Mean	Median	SD	Skew	WHO, 2011
pH	7.57	8.63	8.09	8.05	0.24	0.49	6.5-8.5
TDS	274.37	3618	1075.11	728.13	840.7	1.73	1000 mg/L
TH	155.7	1461.55	374.84	301.4	243.11	2.85	200-600 mg/L
EC	392.03	5169.74	1536.18	1040	1201.27	1.73	1500 ìS/cm
TA	170.68	1015.04	426.56	357.9	221.92	1.2	200-600 mg/L
Na^+	23.62	95.48	49.04	44.88	17.44	1.35	200-400 mg/L
K^+	0.06	1.31	0.49	0.46	0.35	0.73	12 mg/L
Ca^{2+}	28.71	412.64	89.52	69.925	69.64	3.33	75-100 mg/L
Mg^{2+}	16.37	92.47	34.05	29.02	16.18	1.83	30-150 mg/L
F^-	0.05	5.3	0.98	0.34	1.27	1.99	1.5 mg/L
NO_3^-	1.73	278.11	65.24	38.83	63.54	1.4	10-45 mg/L
Cl^-	49.93	1162.6	233.77	132.2	255.49	2.22	200-600 mg/L
HCO_3^-	15.06	845.37	245.2	244.48	162.6	1.2	-
SO_4^{-2}	71.25	124.43	88.21	86.8	8.26	1.49	200-400 mg/L

with 233.77 mg/L of average concentration in the groundwater samples. The Cl^- in the groundwater is mainly originated from the dissolution of halite salt (NaCl) or from atmospheric rain, weathering and leaching of sedimentary rocks, soil and domestic effluents (Prasanth, 2012). Fluoride (F^-) concentration is ranged from 0.05 to 5.3 mg/L with average of 0.98 mg/L in the 24% of groundwater samples of study area, F^- concentration exceeds the acceptable limits of (1.5mg/L). Fluorine mostly accumulates in an alkaline environment (Wu et al., 2015; Chen et al., 2017), higher pH enhances the dissolution of F-bearing minerals due to which excess of F^- is contributed to the groundwater.

Sulphate (SO_4^{-2}) is mainly contributed to the groundwater from the dissolution of gypsum, leaching from fertilizers and municipal wastes (Singh 1994). SO_4^{-2} concentration ranges from 71.25 to 124.43 mg/L with an average of 88.21 mg/L.

In the recent decades, nitrate (NO_3^-) concentration in the groundwater of agricultural regions has increased at higher level due to the intensive use of chemical fertilizer (Wu and Sun, 2016). The NO_3^- ions are mainly contributed from the agricultural fertilizers, animal excreta and nitrification of ammonium to the groundwater. NO_3^- concentration in the study area varies from 1.73 to 278.11 mg/L with mean value of 65.24 mg/L. and in the majority of groundwater samples (84%) is determined beyond the acceptable limit (10 mg/L) (WHO, 2011). The higher nitrate concentration in the study area is reported in the groundwater samples collected from the open wells and the open wells confined within farming land, and located along the drainage courses.

Na^+ and Ca^{2+} are the major cations determined in the groundwater of the study area. The abundance order of the cations is $Na^+ > Ca^{2+} > Mg^{2+} > K^+$. The concentration of Na^+ is ranged from 23.62 to 95.48 mg/L with mean value of 49.04 mg/L. The K^+ ion is the least abundant ion in the major cations and its concentration ranged from 0.06 to 1.31mg/L with average value of 0.49 mg/L. Na^+ contributed to 48.86% of the total cationic charge equivalence (TZ^+), whereas K^+ is less than 1%. In all water samples Na^+ and K^+ concentrations were determined within the acceptable limit set by WHO (WHO, 2011). Na^+ and K^+ in the groundwater are mainly derived from weathering of silicate minerals like albite, orthoclase, microcline and muscovite and additionally from the agricultural sources (Li et al., 2013). However, cation exchange with Ca^{2+} and Mg^{2+} also influences Na^+ and K^+ concentrations in the groundwater (Li et al., 2010).

The Ca^{2+} ion concentration ranged from 28.71 to 412.64 mg/L with mean of 89.52 mg/L. The Ca^{2+} accounted 30.62% to the total cationic charge equivalence (TZ^+). The major sources of calcium in the groundwater are weathering of carbonate, sulphate and silicate minerals. Concentration of Mg^{2+} in the groundwater samples is varied from 16.37 to 92.47 mg/L with mean of 34.05 mg/L and accounted for 20.26% of the TZ^+ charge balance.

Ca^{2+} and Mg^{+2} concentrations are exceeded in the 42% and 44% of the groundwater samples to the acceptable limit of 75 mg/L and 30 mg/L, respectively. Ca^{+2} and Mg^{+2} are usually contributed from the dissolution of carbonate minerals and silicates present in rocks (Berner and Berner, 1987). Though, extensive agricultural activities may also influence the Ca^{+2} and Mg^{+2} concentrations in groundwater (Bohlke, 2002).

In most of the groundwater samples HCO_3^-, SO_4^{2-}, Cl^- contents is determined within the acceptable limits. Cl^- is derived from the weathering, leaching of sedimentary rock and soil, and domestic effluents (Prasanth, 2012), whereas Sulphate is mainly contributed to groundwater from the dissolution of gypsum, leaching from fertilizers and municipal wastes (Singh, 1994).

TA values in 96% groundwater samples is observed above the maximum acceptable limit (200 mg/L), higher values of TA may be due to the dissolution of HCO_3 in groundwater, silicates and rocks weathering processes. Atmospheric CO_2 and CO_2 released from organic decompositions in the soil may also contribute to the increase of HCO_3 concentration in the groundwater (Subba Rao, 2002). Except the weathering and dissolution of minerals, the cations and anions are also contributed from the anthropogenic sources (Hem, 1991; Marghade et al., 2015; Subba Rao et al., 2017).

STATISTICAL ANALYSIS

The correlation between studied physicochemical parameters is evaluated using Pearson's correlation coefficient method and represented in Table 2. The EC and TDS has shown high correlation coefficient with Cl^- (r = 0.96), SO_4^{2-} (r = 0.59), Ca^{2+} (r = 0.75) and Mg^{2+}(r = 0.78) (Table 2) which explicates large participation of these elements towards hydrochemical characteristics of groundwater in the study area (Marghade et al., 2019). Moreover, the positive correlation of TDS with Ca^{2+}, Mg^{2+}, Na^+, K^+, Cl^-, F^- and NO_3^- indicate the involvement anthropogenic input.

A strong positive correlation of TH with Ca^{2+} (r = 0.99), Mg^{2+} (r = 0.93) and Cl^- (r = 0.80) and the strong positive correlation of Ca^{2+} and Mg^{2+} with chloride, Ca^{2+}-Cl^- (r = 0.76), Mg^{2+}-Cl^- (r = 0.80) and negative correlation of Ca^{2+} and Mg^{2+} with bicarbonate, Ca^{2+}-HCO_3^- (r = -0. 24), Mg^{2+}-HCO_3^- (r = -0. 25) suggest that the hardness is mainly due to the chlorides of Ca^{2+} and Mg^{2+}. Additionally, in the 78.7% of the groundwater samples TH is determined higher than that of the TA, which suggests that the hardness is noncarbonated hardness type, which cannot be removed easily from the waters (Chow, 1964). The positive correlation of Ca^{2+} with Cl^- (r = 0.75) and NO_3^- (r = 0.41) indicates about the increased level of pollution in the groundwater (Table 2). This is further evidenced by positive correlation of NO_3^- with Cl^- (r = 0.54).

The negative correlation between SO_4^{2-} and HCO_3^- (r = –0.19)

Table 2. Correlation analysis data's for groundwater samples

Parameters	TDS	F^-	pH	TH	EC	NO_3^-	Cl^-	HCO_3^-	TA	Na^+	K^+	Ca^{2+}	Mg^{2+}	SO_4^{-2}
TDS	1.00													
F^-	0.36	1.00												
pH	-0.01	0.70	1.00											
TH	**0.78**	-0.06	-0.43	1.00										
EC	**0.99**	0.36	-0.01	**0.78**	1.00									
NO_3^-	0.59	0.24	-0.07	0.46	0.59	1.00								
Cl^-	**0.96**	0.18	-0.13	0.80	**0.96**	0.54	1.00							
HCO_3^-	0.05	0.64	0.56	-0.25	0.05	-0.11	-0.10	1.00						
TA	0.38	0.83	0.73	-0.10	0.38	0.23	0.19	0.56	1.00					
Na^+	0.14	-0.18	-0.10	0.18	0.14	0.21	0.16	-0.18	-0.03	1.00				
K^+	0.25	0.43	0.32	-0.02	0.25	0.22	0.14	0.31	0.50	0.01	1.00			
Ca^{2+}	**0.75**	-0.06	-0.44	**0.99**	**0.75**	0.41	**0.76**	-0.24	-0.12	0.12	-0.01	1.00		
Mg^{2+}	**0.78**	-0.06	-0.38	**0.93**	**0.78**	0.58	**0.82**	-0.25	-0.04	0.33	-0.03	0.88	1.00	
SO_4^{-2}	-0.19	-0.26	-0.15	-0.03	-0.19	-0.17	-0.15	-0.28	-0.21	-0.21	-0.01	0.02	-0.16	1.00

advises that the SO_4^{2-} and HCO_3^- ions have different sources. The positive correlation of F^- with pH (r = 0.70), HCO_3^- (r = 0.64) and TA(r = 0.83) indicates that the alkaline environmental condition has favored to the leaching of F^- bearing rocks due to which F^- content in groundwater is surpassed (Subba Rao, 2011).

The positive correlation of F^- with pH (r = 70) and HCO_3 (r = 0.64) suggest the feldspar or fluorapatite may be the source of fluoride. Negative correlation of F^- with Ca^{+2} (r = -0.06) and Mg^{+2} (r = -0.06) is favoring the precipitation of Ca^{2+} and Mg^{+2} from groundwater as a CaF_2 and MgF_2 due to excess of Ca^{2+} and Mg^{+2} in groundwater (Li et al., 2018).

The strong positive correlations of Cl^- with EC (r = 0.96), TDS (r = 0.96) and TH (r = 0.78) indicate anthropogenic inputs for Cl^- enhancement in the groundwater. The minor positive correlation between NO_3^- with Ca^{2+} (r = 0.41), NO_3^- with Mg^{2+} (r = 0.58), NO_3^- with Na^+ (r = 0.21) and NO_3^- with K^+ (r = 0.22) supporting that nitrate is contributed from some nitrate bearing minerals also.

The strong positive correlation between EC and TDS (r = 0.99) indicate the dissolution of more dissolved inorganic ions increases the electrical conductance of the groundwater samples (Alam et al., 2020) and the correlation of TDS and EC with Cl^- (r = 0.96), Ca^{2+} (r = 0.75), Mg^{2+} (r = 0.78) and TH (r = 0.78), and significant positive correlation with NO_3^- (r = 0.59) reflects the anthropogenic influences (Han and Liu, 2004). The strong correlations of TDS and EC with cations Ca^{2+} (r = 0.75), Mg^{2+} (r = 0.78) and anion Cl^- (r = 0.96), and minor positive correlations with Na^+, K^+, NO_3^- and F^- confirm the role of anthropogenic activities in addition to geogenic origin of these ions. Furthermore, the significant positive correlation between F^--NO_3^- (r = 0.24), F^--K^+ (r = 0.43), and Na^-–NO_3^- (r = 0.21) is indicated that the human influence is enriching these ions in the groundwater. Moreover, the Cl^-–NO_3^- (r = 0.54) correlation is supportive of anthropogenic sources of NO_3^- and Cl^- ions from the leachate of dumping site and punctured sewer pipelines (Zakhem and Hafez, 2015).

Hydrogeochemical Evolution of Groundwater

The halite dissolution liberates equal number of Na^+ and Cl^- ions into the solution (Anantha and Chandrakanta, 2014). Thus, Na^+/Cl ratio should be unit and a linear relationship is anticipated between Na^+ and Cl^- ions. In the groundwater of the study area Na^+/Cl^- molar ionic ratios for the majority of groundwater samples is determined more than 1(avg.=1.82), and large number of the groundwater sampling points are plotted above the (1:1) equiline in Na^+ versus Cl^- relation plot (Fig. 3a), suggesting that silicate weathering and ion exchange process are the major sources of Na^+ and Cl^- in groundwater. Additionally, the poor correlation of Na^+ with Cl^- (r = 0.16) (Table 2), and low Na^++K^+ / total cations (TZ^+) ratio (avg. 0.5) (Fig. 3b) confirms that the silicate weathering and ion exchange process are the dominant natural processes, which are contributing Na^+ ions to the groundwater.

Also, the contribution of Na^+ and K^+ from the silicate weathering can be anticipated by the ratios of (Na^++K^+)/TZ^+ (Total cations) (Stallard and Edmond, 1983). The water samples fall below the 0.5 TZ^+ equiline indicative of low silicate weathering while the samples be inclined towards the (Na^++K^+) = TZ^+ line signifies the domination of silicate weathering. It is evident from the bivariate plot of (Na^++K^+) versus TZ^+ (Fig. 3b) that few samples lie below the 0.5 TZ^+ equiline have lower influence of silicate weathering while the majority of samples fall above or along the 0.5 TZ^+ line signifying the dominance of silicate weathering.

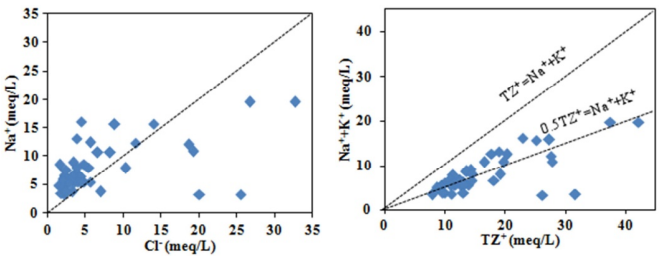

Fig. 3. The bivariate plot of **(a)** Na^+ vs. Cl^-. **(b)** (Na^++K^+) vs. TZ^+ (Total cations).

The negative correlation of HCO_3^- with Ca^{2+} (r = -0.24) and Mg^{2+} (r = -0.25), and higher (Ca^{2+} +Mg^{2+})/HCO_3^- ratio (avg. 5.06) of groundwater samples reflecting that the dissolution of carbonates is not a sole source of Ca^{2+} and Mg^{2+}. An excess of (Ca^{2+} + Mg^{2+}) over HCO_3^- signifying that Ca^{2+} and Mg^{2+} are also contributed from the non-carbonate sources such as weathering of Ca–Mg-rich silicates, dissolution of gypsum, reverse ion exchange and anthropogenic inputs.

The scatter plot of (Ca^{2+}+Mg^{2+}) and (HCO_3^- + SO_4^{2-}) (Fig. 4a) illustrates the occurrence of calcite, dolomite and gypsum dissolution in the groundwater system. The samples plot along the equiline (1:1) represents the dominance of calcite and gypsum weathering processes. For the current study, 60% of the data points of the groundwater samples fall above the equiline (1:1) of the plot indicates an excess of Ca^{2+} and Mg^{2+} over HCO_3^- and SO_4^{2-} with the dominance of carbonate dissolution, while 40% of the data points fall below the equiline (1:1) of the plot shows an excess of HCO_3^- and SO_4^{2-} over Ca^{2+} and Mg^{2+} (Fig. 4a) in which silicate weathering and ion exchange processe are dominated. The excess of HCO_3^- and SO_4^{2-} may be balanced by the Na^+ and K^+, suggested a contribution of Ca^{2+} and Mg^{2+} from non-carbonate source.

Also, in the bivariate plot of (Ca^{2+}+Mg^{2+}) versus HCO_3^- (Fig. 4b), 60% of groundwater sampling points fall above the 1:1 equiline, represents the excess of (Ca^{2+}+Mg^{2+}) over HCO_3^-, which is suggestive of non-carbonate sources of Ca^{2+} and Mg^{2+} in groundwater and demanding other anions i.e. SO_4^{2-} and Cl^- to balance the excess of alkaline earth metal ions in water samples. But, in 40% of water samples which fall below equiline show the excess of HCO_3^- over (Ca^{2+}+Mg^{2+}) indicates the dominance of silicate weathering. Moreover, (Ca^{2+}+Mg^{2+}) / HCO_3^- ratios for majority of the samples greater than one (avg. 5.04) indicate that carbonate weathering is dominated.

The Ca^{2+} and SO_4^{2-} ions concentration in groundwater may be increased by gypsum. In the bivariate plot of Ca^{2+} versus SO_4^{2-} (Fig. 4c), majority of data points fall below the equiline (1:1), Ca^{2+}/ SO_4^{2-} ratios for all the samples is more than one with mean of 2.73, suggesting that the gypsum dissolution also contributing Ca^{2+} and SO_4^{2-} ions to the groundwater.

In this way, the similar ratios of (Na^++K^+)/TZ^+ (0.5) and (Ca^{2+}+Mg^{2+})/ TZ^+ (0.5), and lower ratios of HCO_3^-/(Cl^-+SO_4^{2-}) (0.69) and HCO_3^-/(HCO_3^-+SO_4^{2-}), suggested that the silicate weathering and carbonate dissolution are the providers of dissolved ions in the groundwater of study area.

The Ca^{2+} versus HCO_3^- bivariate plot demonstrates the effect of cation exchange, chemical weathering, and evaporation in the groundwater. In the groundwater calcite is only source of Ca^{2+} and HCO_3^-, the equivalent ratio of dissolved Ca^{2+} and HCO_3^- is 1:2, if dolomite is sole source than the equivalent ratio is 1:4 (Sonkamble et al., 2012). The bivariate plot of Ca^{2+} versus HCO_3^- (Fig. 4d) illustrates that the majority of the data points of groundwater are lay above the 1:2 line indicating the calcite dissolution is main contributor of Ca^{2+} and HCO_3^-, only one sampling point is located near (1:4) line suggesting the dominance of dolomite dissolution.

Additionally, in the Ca^{2+} versus HCO_3^- half of the sampling points fall above the 1:1 equiline, signifying the excess of Ca^{2+} over HCO_3^- which are suggestive of non-carbonate sources of Ca^{2+} and Mg^{2+} in groundwater and demanding other anions i.e. SO_4^{2-} and Cl^- to balance the excess of alkaline earth metal ions in water samples. Relatively

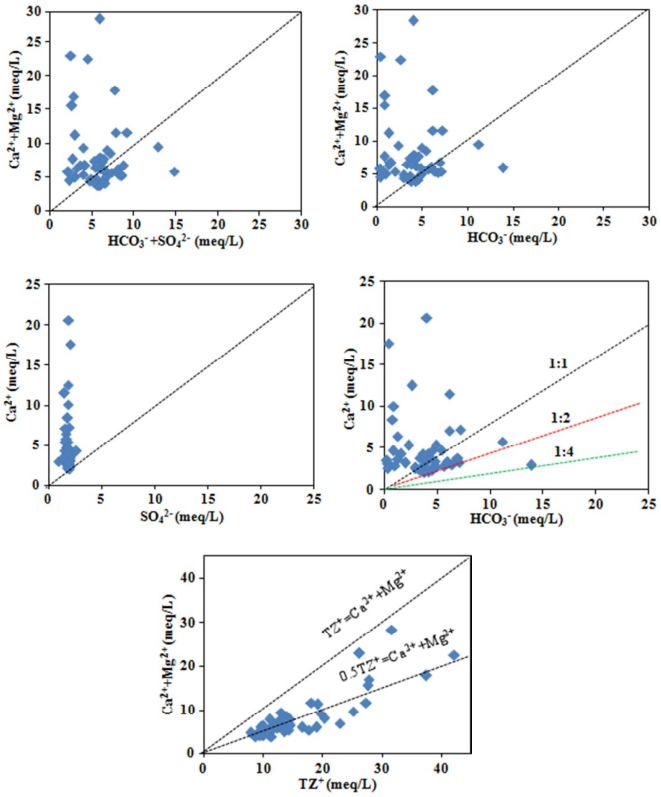

Fig. 4. The bivariate plot of **(a)** (Ca^{2+} +Mg^{2+}) vs. (HCO_3^- + SO_4^{2-}). **(b)** (Ca^{2+} + Mg^{2+}) vs. HCO_3^- . **(c)** Ca^{2+} vs. SO_4^{2-}. **(d)** Ca^{2+} vs. HCO_3^-. **(e)** (Ca^{2+}+Mg^{2+}) vs. TZ^+ (Total cations)

higher ratios in these samples indicate other sources of Ca^{2+} and Mg^{2+} ions, such as reverse cation exchange and/or gypsum dissolution (Zhou et al., 2020). Half of the samples plot below the equiline 1:1 that reveals the excess of HCO_3^- over (Ca^{2+}+Mg^{2+}) or Ca^{2+} suggest the existence of silicate weathering. The depletion of Ca^{2+} and Mg^{2+} in the aquifers may be caused by the cation exchange processes. Ca^{2+}/Mg^2 ratios for 92% of groundwater samples is more than one, for one sample Ca^{2+}/Mg^2 <1 and for three samples Ca^{2+}/Mg^2 >2, indicates the dominance of calcite dissolution.

The role of silicate weathering towards the contribution of alkaline earth metal ions can be estimated from the bivariate plot of (Ca^{2+}+Mg^{2+}) versus TZ^+. When groundwater sampling points fall along the (Ca^{2+}+Mg^{2+}) = TZ^+) line of (Ca^{2+}+Mg^{2+}) versus TZ^+ bivariate plot (Fig. 4e) show the weathering of calcium and magnesium-rich minerals and data points lie below the (Ca^{2+}+Mg^{2+}) = 0.5 TZ^+ line reveal the lower influence of silicate weathering. The samples from the study area fall below and above the (Ca^{2+}+Mg^{2+}) = 0.5 TZ^+ line of (Ca^{2+}+Mg^{2+}) versus TZ^+ plot indicating the influence of silicate weathering (Fig.4e).

The excess of Ca^{2+}+Mg^{2+} over HCO_3^- +SO_4^{2-} in groundwater samples is due to reverse ion exchange process, while the excess of HCO_3^- and SO_4^{2-} may be resulted by ion exchange process and influenced by silicate weathering (Tay et al., 2015).

The major lithological processes that generally undergo chemical weathering are carbonates, silicates, and evaporites. The dominance of these process can be fixed appropriately considering the ratios of Ca^{2+}/Na^+, Mg^{2+}/Na^+, and HCO_3^-/Na^+. As shown in the bivariate plots of Ca^{2+}/Na^+ versus HCO_3^-/Na^+ (Fig. 5a) and Ca^{2+}/Na^+ versus Mg^{2+}/Na^+ (Fig. 5b), the majority of the groundwater samples are plotted in the transitional area between the carbonate end-member and silicate weathering that reveals the influence of both the silicate weathering and carbonate dissolution.

Ion Exchange Process

Ion exchange is the process by which exchange of ion occurs between groundwater and the aquifer environment during residence and movement time. It can be explained through the study of alkaline chlorine indices (Raju et al., 2011). During the ion exchange process exchange of alkali metal cations in the rock take place with alkaline earth metal (Mg^{2+} and Ca^{2+}) cations in the water and vice versa. Positive CAI indicates the exchange of Na^+ and K^+ in water with Mg^{2+} and Ca^{2+} of the rocks, while the negative indicates that there is an exchange of Mg^{2+} and Ca^{2+} in the water with Na^+ and K^+ of the rocks (Mahmoudi et al., 2017). Equations (1) and (2) express the CAI. The concentrations are in meq/L:

$$\text{CAI-I} = \frac{Cl^- - (Na^+ + K^+)}{Cl^-} \quad (1)$$

$$\text{CAI-II} = \frac{Cl^- - (Na^+ + K^+)}{SO_4^{2-} + HCO_3^- + NO_3^- + CO_3^{2-}} \quad (2)$$

CAI values for the majority of groundwater samples (82%) of the study area are negative, which suggested that the Mg^{2+} and Ca^{2+} present in the groundwater are exchanged with the Na^+ and K^+ ions present in the rocks at the surface of rocks. It represents cation–anion exchange reaction or chloro-alkaline disequilibrium with dominance of ion exchange. Whereas for remaining samples, CAI values are determined positive, that indicated the exchange of Na^+ and K^+ ions present in water with Ca^{2+} and Mg^{2+} ions at the surface of aquifer material. This results an excess of Ca^{2+} and Mg^{2+}

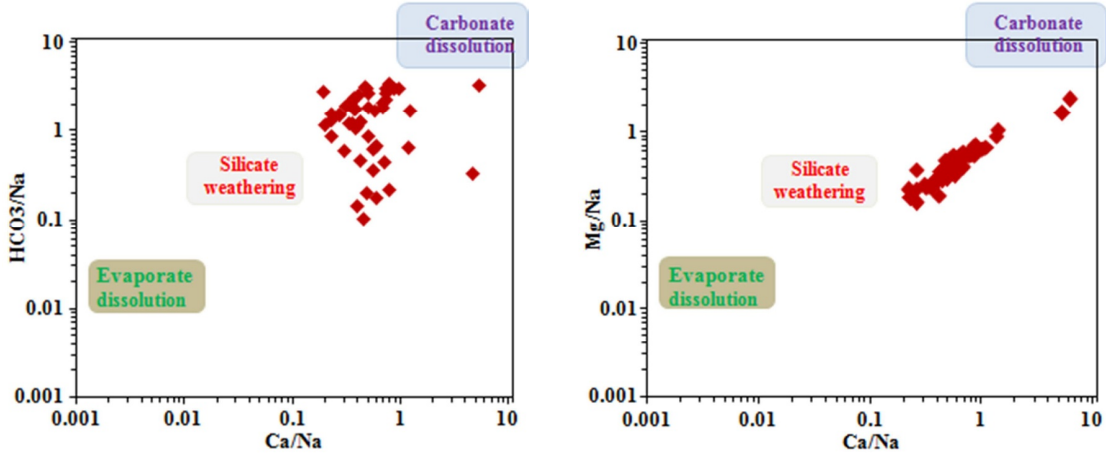

Fig.5. The bivariate plot of **(a)** HCO_3^- / Na^+ versus Ca^{2+}/Na^+. **(b)** Mg^{2+} / Na^+ versus Ca^{2+}/Na^+

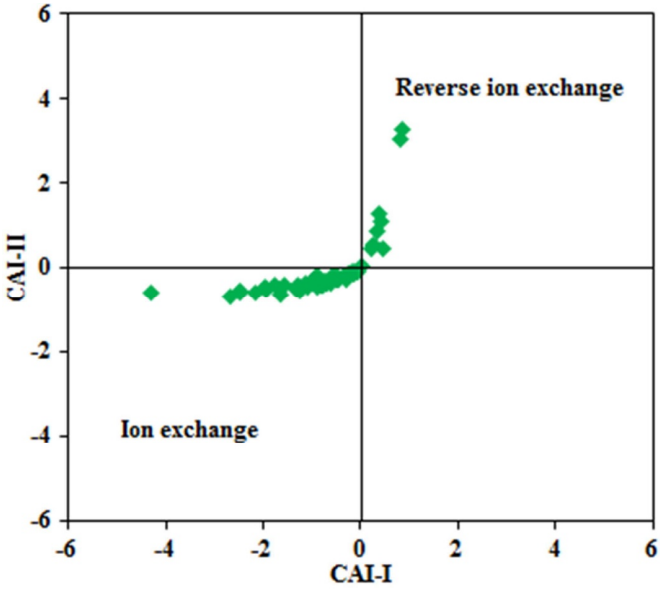

Fig.6. The relation plot between CAI-I and CAI-II.

concentration in water. It represents direct base-exchange reaction or chloro-alkaline equilibrium with the dominance of reverse ion exchange process.

As shown in Fig. 6, most of the groundwater sampling points in the relation plot drawn between CAI-I and CAI-II, are located in reverse ion exchange region confirm the dominance reverse ion exchange process in groundwater of study area (Hao et al., 2020). The ratios of $(SO_4^{2-} + HCO_3^-)/(Ca^{2+}+Mg^{2+})$ less than one advocates the dominance of carbonate weathering and reverse ion exchange process with the excess of $(Ca^{2+}+Mg^{2+})$ over $(SO_4^{2-}+HCO_3^-)$ as shown in Fig. 4a (Gogoi et al., 2021; Fisher and Mulican, 1997). Additionally, the bivariate plot of $(Na^++K^+) - Cl^-$ versus $(Ca^{2+}+Mg^{2+}) - (SO_4^{2-} + HCO_3^-)$ (Fig. 7), also confirm the dominance of reverse ion exchange over the ion exchange process in majority of the groundwater samples.

Saturation State of Groundwater - Saturation Indices (SI)

In order to take place any geochemical reaction, there must be disequilibrium between water and mineral phases. The equilibrium

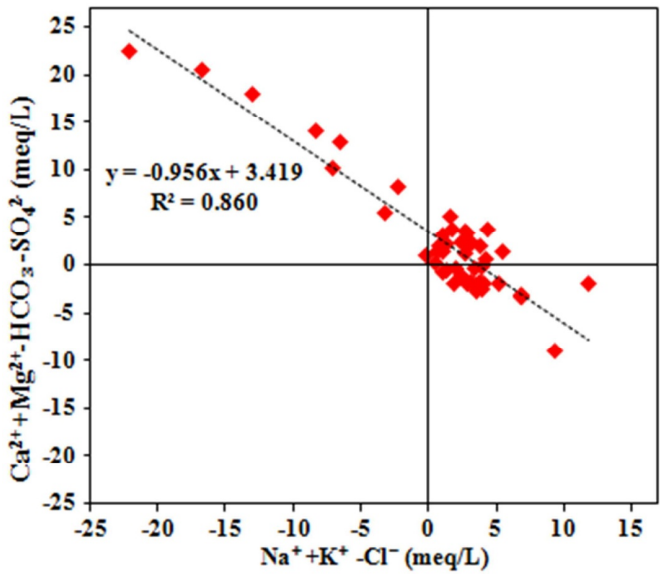

Fig.7. The bivariate plot of $(Na^++K^+) - Cl^-$ versus $(Ca^{2+}+Mg^{2+})-(SO_4^{2-} + HCO_3^-)$

state can be measured by estimating the saturation indices. Saturation indices (SI) with respect to calcite, dolomite, aragonite and gypsum minerals were calculated using the following equation (3).

$$SI = \log_{10} (K_{IAP} / K_{Sp}) \quad (3)$$

where, SI is the saturation index, K_{IAP} is the ionic activity product of the ions, K_{Sp} is the solubility product of the mineral. The positive value of SI depicts the over saturation state of water, while negative value indicates under saturation state. At over saturation condition, the mineral phase precipitates whereas at under saturation it dissolves at equilibrium (Tiwari et al., 2021).

The super saturation leads to precipitation of calcite and dolomite. The plot of SI(calcite) versus SI(dolomite) (Fig. 8a) discloses that 90% of the groundwater samples are over saturated with reference to dolomite and calcite and the SI(dolomite) values are higher than that of the SI(calcite) values. However, five samples of the study area have negative SI indices which reveal that the groundwater is under saturation state with reference to dolomite and calcite. The under saturation could lead to the dissolution of dolomite and calcite in water during interaction with mineral rocks. Moreover, all the samples with reference to gypsum are undersaturated that lead to dissolution of gypsum in the groundwater until the equilibrium conditions altered and 90 % of samples are oversaturated concerning to aragonite that favour precipitation (Fig 8b).

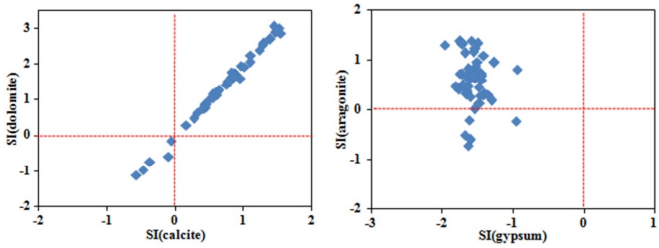

Fig.8. Relation between **(a)** SI(dol) and SI(cal). **(b)** SI(gyp) and SI(arg)

Water Types

The hydrogeochemically the groundwater can be categorized into different types upon the basis of various diagrams such as Piper (1944), Chadha (1999), Durov (1948) and Schoeller (1964) diagrams. As shown in Piper diagram (Fig. 9), the groundwater samples are predominantly of the Ca.Mg-HCO_3 type followed by Ca.Mg-Cl and Ca.Mg–SO_4 type. The dominance of Ca.Mg-HCO_3 type is clearly indicating that the sufficient recharge from fresh water with temporary hardness, while the existence of Ca.Mg-Cl and Ca.Mg–SO_4 type of water reflecting the presence of permanent hardness (Handa, 1979).

It is evident from the modified Piper diagram proposed by Chadha (1999) as shown in Fig.10, 52 % of the groundwater samples are located in the field with exceeding of strong acidic anions compare to weak acidic anions. Moreover, in the majority of the groundwater samples alkaline earth metal ions are exceeding to the alkali metal ions that also confirm the existence of Ca.Mg-HCO_3, Ca.Mg-Cl and Ca.Mg-SO_4 type of waters. Additionally, the existence of Ca.Mg-HCO_3 type of water indicating the recharge of the groundwater from the surface water with dissolved carbonates in the form of HCO_3 and geologically mobile Ca^{2+} and Mg^{2+}, Ca.Mg-Cl type water shows that the effect of evaporation and human activities on the groundwater chemistry and also reflect occurrence of the reverse ion exchange which results into excess of $(Ca^{2+} + Mg^{2+})$ over $(Na^+ + K^+)$.

In the Durov diagram (Fig. 11), 86% of groundwater sampling points in reference to cations are plotted in no dominance zone of left

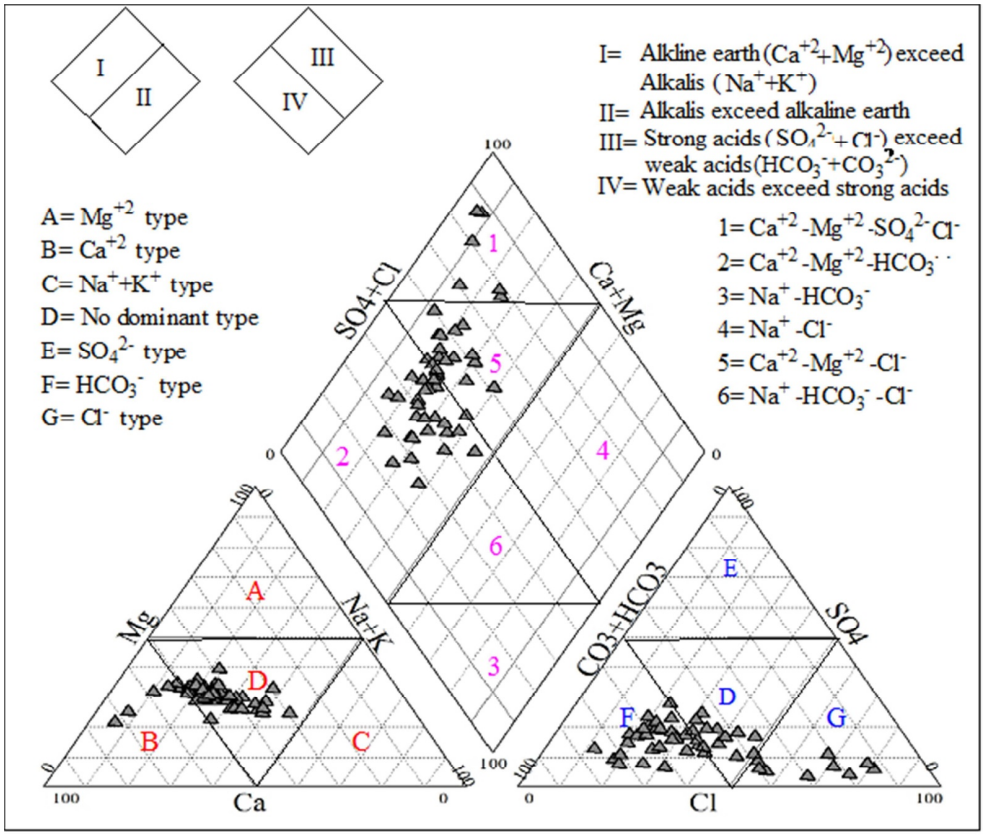

Fig.9. Piper diagram for groundwater samples.

triangle, and remaining in Ca-zone, suggesting that the groundwater is mixed and Ca-type.

On the contrary, with respect to anions, 54% samples are plotted in no dominant zone in the upper triangle of the Durov diagram which shows the dominance of the mixed type water, in the 17 and 11 samples, HCO_3 and Cl-type of groundwater is observed. In reference to TDS, 66% groundwater samples in the Durov diagram are plotted below TDS < 1000 mg/L which are characterized as fresh water types. The other samples are belonged to the brackish water group with the sulfate and mixed water type, indicating the combine influence of evaporation, water–rock interaction, and/or human activities.

Schoeller (1964) diagram (Fig. 12), suggesting that the HCO_3^- and Ca^{2+} are the dominant anion and cation in the groundwater samples and also indicating that the Ca^{2+} and Mg^{2+} are exceeded to the Na^+ and K^+, and Cl^- and HCO_3^- exceeded to the SO_4^{2-} and CO_3^{2-} ions. Thus, the groundwater is classified as Ca.Mg-HCO_3 and Ca.Mg-Cl types.

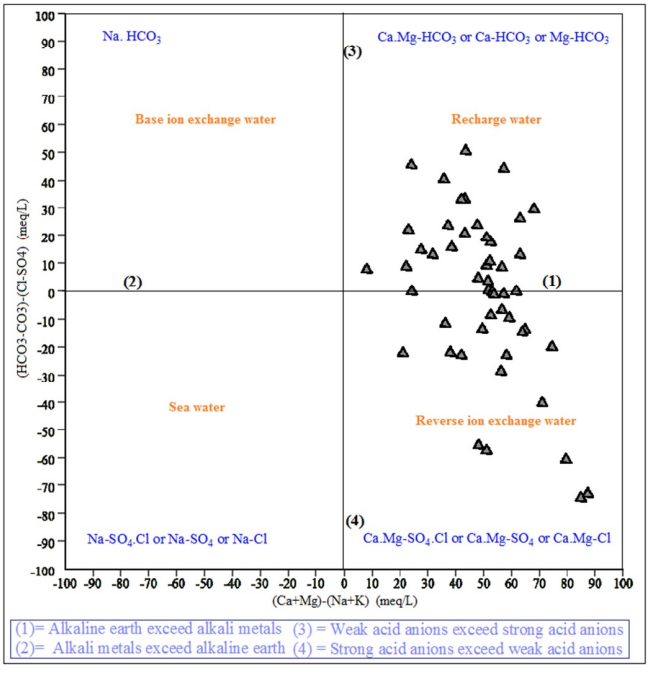

Fig.10. Chadha diagram for groundwater samples

Hydrogeochemical Processes Governing Groundwater Chemistry-Gibb's Diagram

According to the Gibbs (1970), three major hydrogeochemical processes which govern the chemistry of natural water (a) evaporation-crystallization, (b) rock-water interactions and (c) atmospheric precipitation. The Gibbs diagrams (Gibbs, 1970) represent TDS a function of ratio of $(Na^+ + K^+)/(Na^+ + K^+ + Ca^{2+})$ and $Cl^-/(Cl^- + HCO_3^-)$ are widely used to evaluate the contribution of each of the three major processes on water quality (Wanda et al., 2021; Li et al., 2013; Wu et al., 2015; Subba Rao and Surya Rao, 2009).

The Gibbs plots as shown in (Fig. 13 and Fig. 14), the groundwater samples of the study area are scattered from the rock water interaction dominance zone to evaporation dominance zone, which reveals that the hydrochemistry of the groundwater samples is influenced by the rock-water interaction processes with the intrusion of anthropogenic activities. The diffusion of ratios of $(Na^+ + K^+)/(Na^+ + K^+ + Ca^{2+})$ and $Cl^-/(Cl^- + HCO_3^-)$ with high levels of mineralization (TDS) towards the zone of evaporation from the rock dominance is due to increase of Na^+ and Cl^- ion concentrations by anthropogenic sources (Subba Rao and Surya Rao, 2009).

CONCLUSIONS

In summary, the groundwater of the study area is slightly alkaline

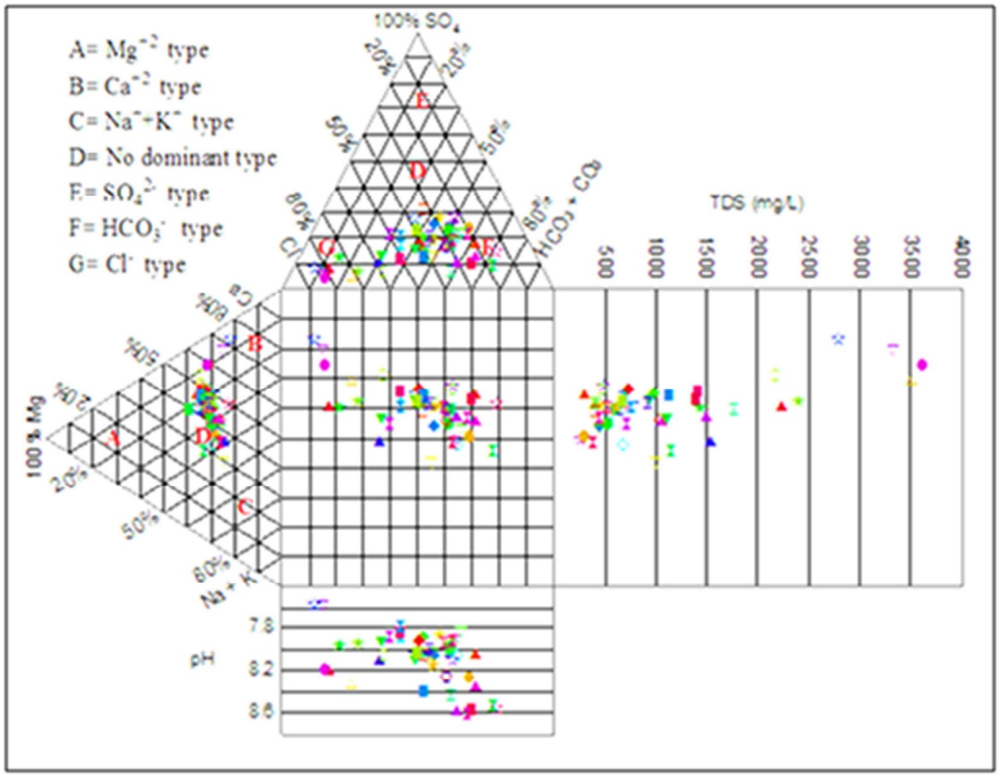

Fig.11. Durov diagram for groundwater samples

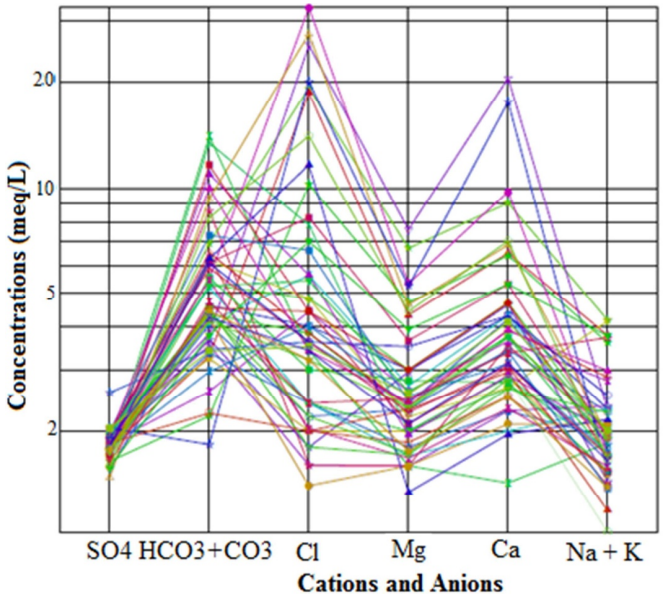

Fig.12. Schoeller diagram for groundwater samples

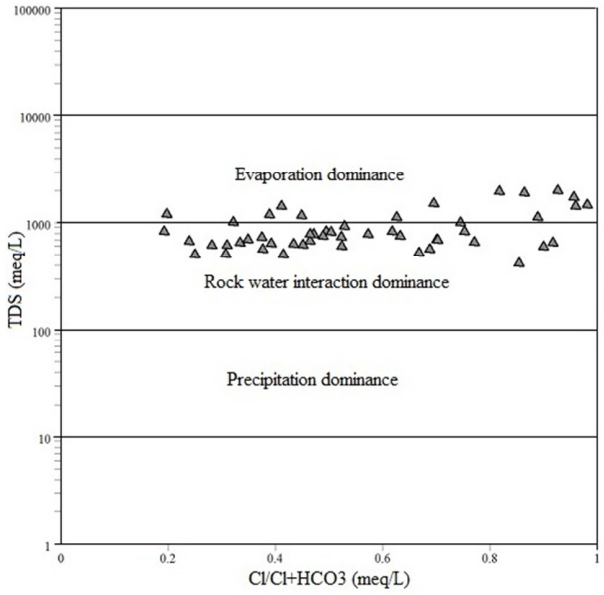

Fig.13. Gibb's diagrams for TDS versus $Cl^-/(Cl^- + HCO_3^-)$

in nature, fresh to fresh brackish (TDS) and hard to very hard (TH), abundance order of major ions was found to be in the order of $Na^+ > Ca^{2+} > Mg^{2+} > K^+$ and $HCO_3^- > Cl^- > SO_4^{2-} > NO_3^- > F^-$. In most of the samples quantity of TH, TA, NO_3^-, TDS and EC is exceeded the prescribed WHO limits, however, the values other parameters in majority of the samples is observed within the standards limits for drinking purpose. The correlation analysis suggested that salinity load in the groundwater of the study area is primarily controlled by Cl^-, TH, Ca^{2+}, Mg^{2+} and NO_3^- , TH is due to the presence of chlorides of calcium and magnesium, the anthropogenic and geogenic activities controlled the origin ions and the dissolution of feldspar or fluorapatite may be a possible source of fluoride.

The alkali metal cations in the groundwater are mainly contributed from the dissolution of halite and silicate weathering processes while the alkaline earth metal cations are contributed from the carbonate dissolution in 60% of groundwater samples while in remaining samples silicate weathering is dominating process. In the carbonate dissolution, the calcite dissolution is the major process and groundwater is oversaturated with dolomite, calcite and aragonite and undersaturated to gypsum, and the groundwater is Ca.Mg-HCO_3 type followed by Ca.Mg-.Cl and Ca.Mg-SO_4 types. Additionally, the alkaline earths exceed alkalis, and the weak and strong acid anions have approximately equal representations. The domination of reverse ion exchange process makes excess of $Ca^{2+}$and Mg^{2+} over Na^+ and K^+ in groundwater.

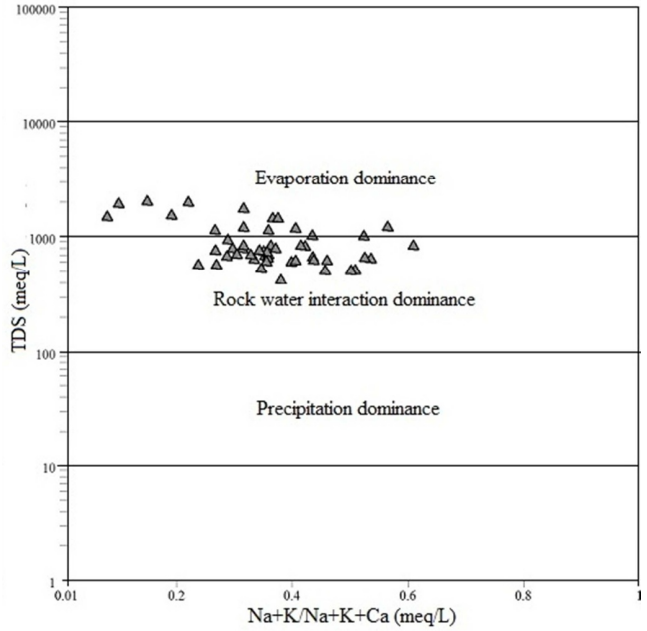

Fig.14. Gibb's diagrams for TDS versus $(Na^+ + K^+)/(Na^+ + K^+ + Ca^{2+})$

Gibb's diagram has suggested that the hydrogeochemistry of the groundwater is mainly governed by the rock water interaction followed by evaporation geological process.

References

Adimalla, N. and Venkatayogi, S. (2018) Geochemical characterization and evaluation of groundwater suitability for domestic and agricultural utility in semi-arid region of Basara, Telangana State, South India. Appl. Water Sci., v.8, pp.44. doi:10.10007/s13201- 018-0682-1

Adrian, H., Gallardo, A. and Tase, Norio (2007) Hydrogeology and geochemical characterization of groundwater in a typical small scale agricultural area of Japan. Jour. Asian Earth Sci., v.29, pp.18–28.

Alam, W., Singh Sonamani, K. , Gyanendra, Y., Laishram Ranu, J. and Nesa, N. (2020) Hydrogeochemical assessment of groundwater quality for few habitations of Chandel District, Manipur (India). Appl. Water Sci., v.10, 123. doi:10.1007/s13201-020-01208-0

An, Y. and Lu, W. (2018). Hydrogeochemical processes identification and groundwater pollution causes analysis in the northern Ordos Cretaceous Basin China. Environ. Geochem. Health, v.40(4), pp.1209–1219.

Anantha, R.V. and Chandrakanta, G. (2014) Major ion chemistry, hydrogeochemical studies and mapping of variability in ground water quality of Sitanadi basin, Southern Karnataka. Octa Jour. Environ. Res., v.2(2), pp.178–196.

APHA (1995) Standard Methods for the Examination of Water and Wastewater, 19th ed. American Public Health Association, Washington, D.C.

Appelo, C. A. J. and Postma, D. (2005) Geochemistry, groundwater and pollution (2nd ed.). Boca Raton, London, New York: CRC Press, Taylor & Francis Group.

Bemer, E. K. and Bemer, R. A. (1987) Water, Air, and Geochemical Cycles (2nd ed.). Princeton and Oxford: Princeton University Press.

Bohlke, J.K. (2002) Groundwater recharge and agricultural contamination. Hydrogeol. Jour., v.10, pp.153–179.

Central Ground Water Board (CGWB, 2010) Ministry of water resources, Government of India.

Chadha, D.K. (1999) A proposed new diagram for geochemical classification of natural waters and interpretation of chemical data. Hydrogeol. Jour., v.7(5), pp.431–439.

Chen, J., Wu, H., Qian, H. and Gao, Y. (2017) Assessing nitrate and fluoride contaminants in drinking water and their health risk of rural residents living in a semiarid region of Northwest China. Expo. Health, v.9, pp.183–195.

Chow, V. T. (1964) Handbook of Applied Hydrology. New York: McGraw-Hill.

Dufor, C.N. and Becker, E. (1964) Public water supplies of the 100 largest cities in the US. Geological Survey Water Supply paper, 1812, 364p.

Duraisamy, S., Govindhaswamy, V., Duraisamy, K., Krishinaraj, S., Balasubramanian A. and Thirumalaisamy, S. (2018). Hydrogeochemical characterization and evaluation of groundwater quality in Kangayam taluk, Tirupur district, Tamil Nadu, India, using GIS techniques. Environ. Geochem. Health, v.41, pp.851–873.

Durov, S.A. (1948) Natural waters and graphical representation of their composition. Doklady Akademii Nauk SSSR, v.59, pp.87–90.

Fisher, R.S. and Mulican III, W.F. (1997) Hydrgeochemical evolution of sodium-sulphate and sodium-chloride groundwater beneath the Northern Chihuahuan desert. Trans- Pecos, Texas USA. Hydrogeol. Jour., v.5(2), pp.4–16. doi:10.1007/ s100400050102.

Freeze, R.A. and Cherry, J.A. (1979) Groundwater. Prentice-Hall, Englewood Cliffs.

Gibbs, R.J. (1970) Mechanisms controlling world water chemistry. Science, v.17, pp.1088–1090.

Gogoi, R.R. Khanikar, L. Gogoi, J. Neog, N. Deka, D.J. and Sarma, K.P. (2021) Geochemical sources, hydrogeochemical behaviour of fluoride release and its health risk assessment in some fluorosis endemic areas of the Brahmaputra valley of Assam, India. Appl. Geochem., v.127, 104911. doi:10.1016/j.apgeochem.2021.104911

Green, T. R. (2016) Linking Climate Change and Groundwater. *In* A.J. Jakeman, O. Barreteau, R.J. Hunt, J.-D. Rinaudo, and A. Ross (Eds.), Integrated Groundwater Management (pp.97–141). Cham: Springer International Publishing. doi:10.1007/978–3–319–23576–9_5.

Han, G. and Liu, C.Q. (2004) Water geochemistry controlled by carbonate dissolution: a study of the river waters draining Karst-dominated terrain, Guizhou province. China. Chem. Geol., v.204(1), pp.21.

Handa, B.K. (1979) Groundwater pollution in India. *In* Proc, National Symp. on Hydrology (pp.34–49). IAHS, Publication University of Roorkee, India.

Hao, C., Zhang, W. and Gui, H. (2020) Hydrogeochemistry characteristic contrasts between low- and high-antimony in shallow drinkable groundwater at the largest antimony mine in hunan province, China. Appl. Geochem., v.117, 104584. doi:10.1016/j.apgeochem.2020.104584

Hem, J.D. (1991) Study and interpretation of chemical characteristics of natural water (263) (3rd ed). USGS Water-Supply Paper 2254.

Iqbal, M.A. and Gupta, S.G. (2009) Studies on heavy metal ion pollution of ground water sources as an effect of municipal solid waste dumping. African Jour.Basic Appl. Sci., v.1, pp.117–122.

Kagan, V.E., Shvedova, A., Serbinova, E., Khan, S., Swanson, C., Powell, R. and Packer, L. (1992) Dihydrolipoic acid—a universal antioxidant both in the membrane and in the aqueous phase: reduction of peroxyl, ascorbyl and chromanoxyl radicals. Biochemical Pharmacology, v.44(8), pp.1637-1649.

Langmuir, D. (1997) Aqueous environmental geochemistry. Upper Saddle River, N.J: Prentice Hall.

Li, P., He, X., Li, Y. and Xiang, G. (2018) Occurrence and health implication of fluoride in groundwater of loess aquifer in the Chinese loess plateau: a case study of Tongchuan, Northwest China. Expo Health, pp.1–13. doi: 10.1007/s12403-018-0278-x.123456789

Li, P., Qian, H., Howard, K.W.F. and Wu, J. (2015) Building a new and sustainable "Silk Road economic belt". Environ. Earth Sci., v.74, pp.7267–7270.

Li, P., Qian, H., Wu, J., Zhang, Y. and Zhang, H. (2013) Major ion chemistry of shallow groundwater in the Dongsheng coalfield, Ordos Basin, China. Mine Water Environ., v.32(3), pp.195–206.

Li, P-Y., Qian, H., Wu, J-H. and Ding, J. (2010) Geochemical modeling of groundwater in southern plain area of Pengyang County, Ningxia, China. Water Sci. Eng., v.3(3), pp.282–291.

Madhav, S., Ahamad, A., Kumar, A., Kushawaha, J., Singh, P. and Mishra, P.K. (2018) Geochemical assessment of groundwater quality for its suitability for drinking and irrigation purpose in rural areas of Sant Ravidas Nagar (Bhadohi), Uttar Pradesh. Geol. Ecol. Landsc., pp.1–10.

Mahmoudi, N. Nakhaei, M. and Porhemmat, J. (2017) Assessment of hydrogeochemistry and contamination of Varamin deep aquifer, Tehran Province, Iran. Environ. Earth Sci., v.76, pp.370.

Marghade, D., Malpe, D.B., Rao, N.S. and Sunitha, B. (2019) Geochemical assessment of fluoride enriched groundwater and health implications from a part of Yavtmal District, India. Hum. Ecol. Risk Assess., pp.1–22. doi:10.1080/10807039.2018.1528862

Marghade, D., Malpe, D.B. and Subba, Rao N. (2015) Identification of controlling processes of groundwater quality in a developing urban area using principal component analysis. Environ. Earth Sci., v.74, pp.5919–5933.

Milovanovic, M. (2007) Water quality assessment and determination of pollution sources along the Axios/Vardar River Southeastern Europe. Desalination, v.213(1–3), pp.159–173. doi:10.1016/j.desal.2006.06.022.

Mohammed, E.A., Aref, L., Nassir, A. and Abdulaziz, A. (2015) Groundwater characteristics and pollution assessment using integrated hydrochemical investigations GIS and multivariate geostatistical techniques in arid areas. Water Resour, Managmt., v.29, pp.5593–5612.

Piper, A.M. (1944) A graphical procedure in the geochemical interpretation of water analysis. Trans. Amer. Geophys. Union, v.25, pp.914–928.

Prasanth, S.V.S., Magesh, N.S., Jitheshlal, K.V., Chandrasekar, N. and Gangadhar, K. (2012) Evaluation of groundwater quality and its suitability for drinking and agricultural usein the coastal stretch of Alappuzha District, Kerala, India. Appl. Water Sci., v.2, pp.165–175.

Qasemi, M., Shams, M., Sajjadi, S. A., Farhang, M., Erfanpoor, S., Youse, M., Zarei, A. and Afsharnia, M. (2019) Cadmium in Groundwater Consumed in the Rural Areas of Gonabad and Bajestan, Iran: Occurrence and Health Risk Assessment. Biol. Trace Elem. Res., v.192, pp.106–115. doi:10.1007/s12011- 019-1660-7

Qian, H., Li, P., Howard, K.W.F., Yang, C. and Zhang, X. (2012) Assessment of Groundwater vulnerability in the Yinchuan Plain, Northwest China using OREADIC. Environ. Monit. Assess., v.184, pp.3613–3628.

Raju, N.J., Shukla, U.K. and Ram, P. (2011) Hydrogeochemistry for the assessment of groundwater quality in Varanasi: a fast-urbanizing center in Uttar Pradesh, India. Environ. Monit. Assess., v.173(1–4), pp.279–300.

Rossiter, H.M.A., Owusu, P.A., Awuah, E., MacDonald, A.M. and Schafer, A.I. (2010) Chemical drinking water quality in Ghana: water costs and scope for advanced treatment. Sci. Total Environ., v.408, pp.2378–2386.

Saeid, S., Chizari, M., Sadighi, H. and Bijani, M. (2018) Assessment of agricultural groundwater users in Iran: a cultural environmental bias. Hydrogeol. Jour., v.26, pp.285-295.

Schoeller, H. (1964) La classification geochimique des waux. I.A.S.H. Publication no. 64. Gen Assembly Berkeley, v.4, pp.16–24.

Singh, K.P. (1994) Temporal changes in the chemical quality of ground water in Ludhiana area. Curr. Sci., v.66, pp.375–378.

Sonkamble, S., Sahya, A., Mondal, N.C., Harikumar, P. (2012) Appraisal and evolution of hydrochemical processes from proximity basalt and granite areas of Deccan Volcanic Province (DVP) in India. Jour. Hydrol., v.181–193.

Subba Rao, N. (2002) Geochemistry of groundwater in parts of Guntur district, Andhra Pradesh, India. Environ. Geol., v.41, pp.552–562.

Subba Rao, N. (2017) Hydrogeology. Problems with Solutions. Prentice Hall of India, New Delhi, India.

Subba Rao, N. and Surya Rao, P. (2009) Major ion chemistry of groundwater in a river basin: A study from India. Environ. Earth Sci., v.61(4), pp.757–775.

Tay, C., Kortatsi, B., Hayford, E. and Hodgsonc, I. (2014) Origin of Major Dissolved Ions in Groundwater within the Lower Pra Basin Using Groundwater Geochemistry, Source- Rock Deduction and Stable Isotopes of ^{2}H and ^{18}O. Environ. Earth Sci., v.71, pp.5079-5097.

Tiwari, A.K. Abhay Singh, K. Phartiyal, B. and Sharma A. (2021) Hydrogeochemical characteristics of the Indus river water system, Chemistry and Ecology, doi: 10.1080/02757540.2021.1999425

Tolera B.M., Choi, H., Chang, S.W., Chung, I-M. (2020) Groundwater quality evaluation for different uses in the lower Ketar Watershed, Ethiopia. Environ. Geochem. Health, doi:10.1007/s10653-019-00508-y

Wanda, E.M.M. Chavula, G. and Tembo, F.M. (2021) Hydrogeochemical characterization of water quality evolution within Livingstonia coalfield mining areas in Rumphi district, northern Malawi. Physics and Chemistry of the Earth, v.123, 103045.

World Health Organization (2011) Guidelines for Drinking Water Quality, 4th ed., WHO, Geneva, Switzerland.

Wu, J. and Sun, Z. (2016) Evaluation of shallow groundwater contamination and associated human health risk in an alluvial plain impacted by agricultural and industrial activities, Mid-West China. Expo. Health, v.8, pp.311–329.

Wu, J., Li, P. and Qian, H. (2015) Hydrochemical characterization of drinking groundwater with special reference to fluoride in an arid area of China and the control of aquifer leakage on its concentrations. Environ. Earth Sci., v.73(12), pp.8575–8588.

Zakhem, B.A. and Hafez, R. (2015) Hydrochemical, isotopic and statistical characteristics of groundwater nitrate pollution in Damascus Oasis (Syria). Environ. Earth Sci., v.74, pp.2781–2797.

Zhou, Y., Li, P., Xue, L., Dong, Z. and Li, D. (2020) Solute geochemistry and groundwater quality for drinking and irrigation purposes: a case study in Xinle City, North China. Geochemistry.